Supporting Information

Electrochemical Switching of Plasmonic Colors Based on Polyaniline-Coated Plasmonic Nanocrystals

Wenzheng Lu,[†] Tsz Him Chow,[†] Sze Nga Lai,[‡] Bo Zheng,[‡] and Jianfang Wang*[†]

[†]Department of Physics, The Chinese University of Hong Kong, Shatin, Hong Kong SAR, China
[‡]Department of Chemistry, The Chinese University of Hong Kong, Shatin, Hong Kong SAR, China
*Email: jfwang@phy.cuhk.edu.hk

Chromaticity Calculation. To determine the CIE chromaticity values of the colors generated from the plasmonic nanocrystals, the coordinates were calculated using the experimental scattering spectra and the color-matching functions[1] defined by the CIE 1931. The spectral power distribution is given by

$$P(\lambda) = I(\lambda)S(\lambda) \tag{1}$$

where $I(\lambda)$ is the relative radiance spectrum of the incident light source, and $S(\lambda)$ is the measured scattering spectrum. The tristimulus values X, Y and Z were calculated according to

$$X = \int P(\lambda)\bar{x}(\lambda)d\lambda \tag{2}$$

$$Y = \int P(\lambda)\bar{y}(\lambda)d\lambda \tag{3}$$

$$Z = \int P(\lambda)\bar{z}(\lambda)d\lambda \tag{4}$$

where $\bar{x}(\lambda)$, $\bar{y}(\lambda)$ and $\bar{z}(\lambda)$ are the color-matching functions for the red, green and blue colors, respectively. They are defined by the CIE standard observers. In order to transform the tristimulus values X, Y and Z into the CIE chromaticity space, the color coordinates (x,y,z) are obtained by normalization

$$x = \frac{X}{X+Y+Z} \tag{5}$$

$$y = \frac{Y}{X+Y+Z} \tag{6}$$

$$z = \frac{Z}{X+Y+Z} = 1 - x - y \tag{7}$$

Only two values, x and y, are independent because of the normalization of the incident light intensity. The calculated coordinates are listed in the table below.

Table S1. Color Coordinates Calculated from the Scattering Spectra and the Color-Matching Functions
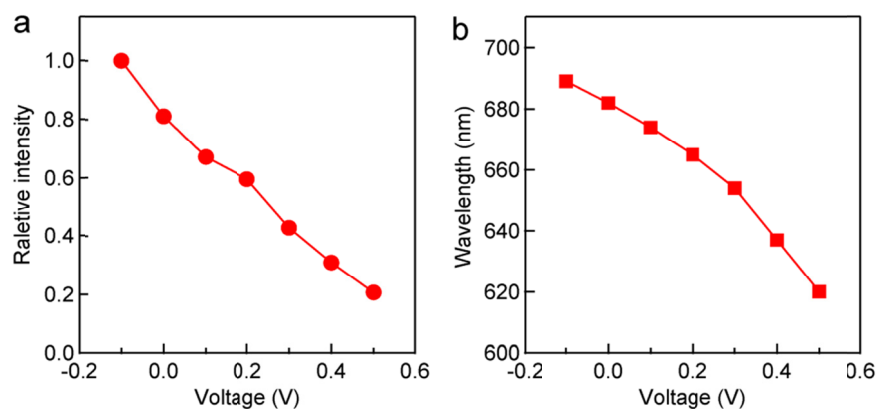
| sample	x	y
Ag NC 1	0.164	0.123
Ag NC 2	0.238	0.352
Au NS 1	0.309	0.570
Au NS 2	0.418	0.483
Au NR 1	0.485	0.425
Au NR 2	0.573	0.370
Au NR 3	0.621	0.342
Au NR 4	0.619	0.336
Au NR 5	0.623	0.330
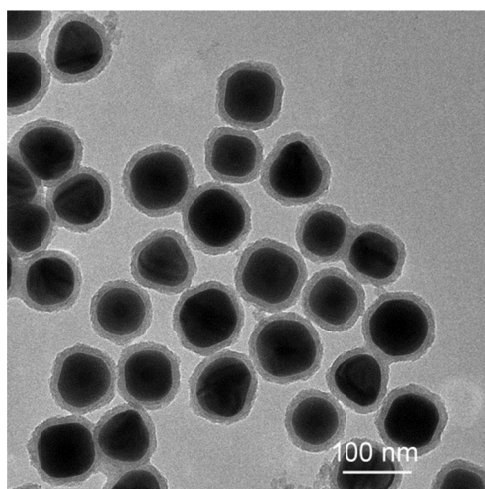
**Figure S1.** TEM image of the silica-coated Ag NC 1 sample.
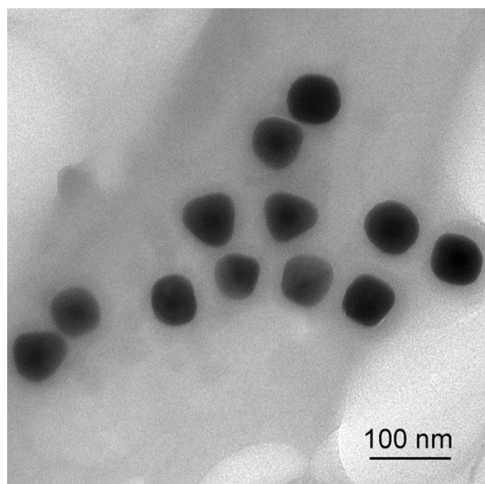
**Figure S2.** TEM image of the PANI-coated Ag NCs.

Figure S3. Electrochemical switching on the PANI-coated Au NRs. (a) Scattering intensity of the longitudinal plasmon for the same single PANI-coated Au NR as shown in Figure 3a as a function of the applied electrochemical potential. The intensities were normalized by dividing them with the scattering intensity at the reduced state. (b) Longitudinal plasmon wavelengths of the PANI-coated Au NR at different applied electrochemical potentials.
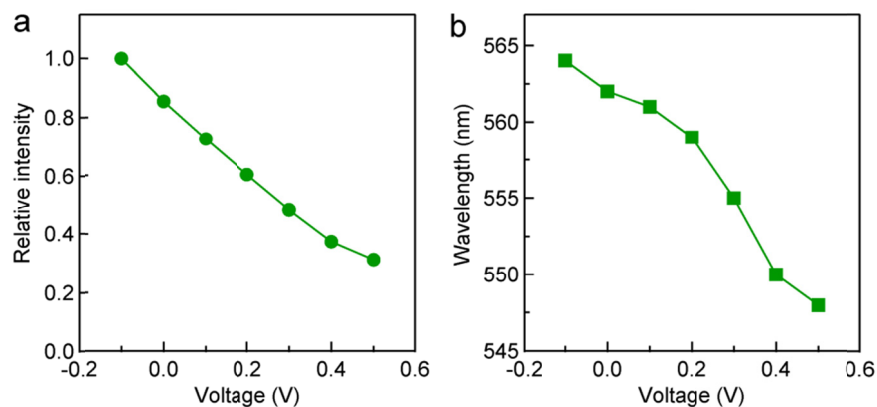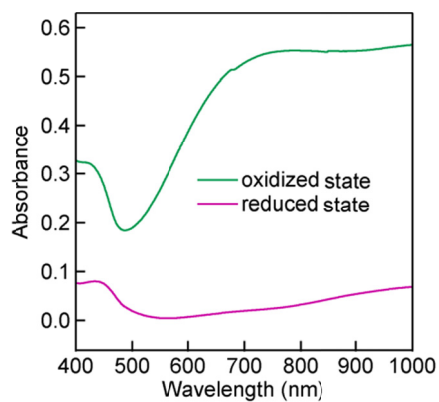
Figure S4. Electrochemical switching on the PANI-coated Au NSs. (a) Scattering intensity of the same single PANI-coated Au NS as shown in Figure 3d as a function of the applied electrochemical potential. The intensities were normalized by dividing them with the scattering intensity at the reduced state. (b) Plasmon wavelengths of the PANI-coated Au NS at different applied electrochemical potentials.
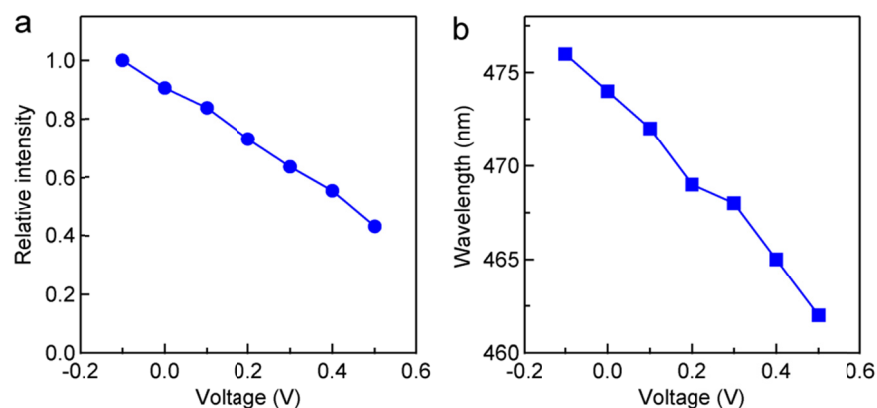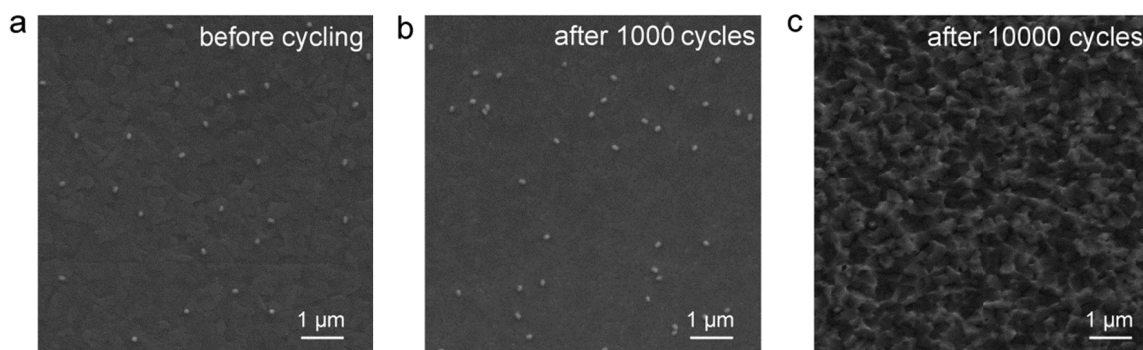

Figure S5. Electrochemical switching on the PANI-coated Ag NCs. (a) Scattering intensity of the same single PANI-coated Ag NC as shown in Figure 3g as a function of the applied electrochemical potential. The intensities were normalized by dividing them with the scattering intensity at the reduced state. (b) Plasmon wavelengths of the PANI-coated Ag NC at different applied electrochemical potentials.
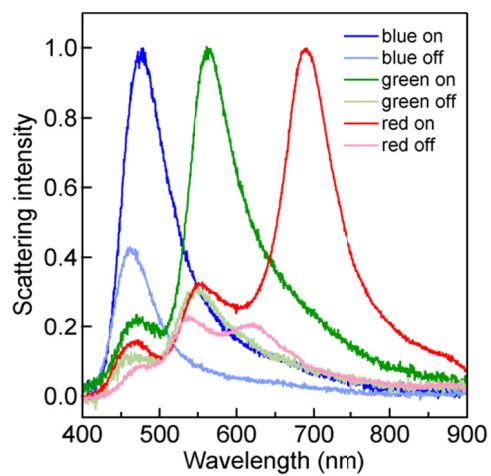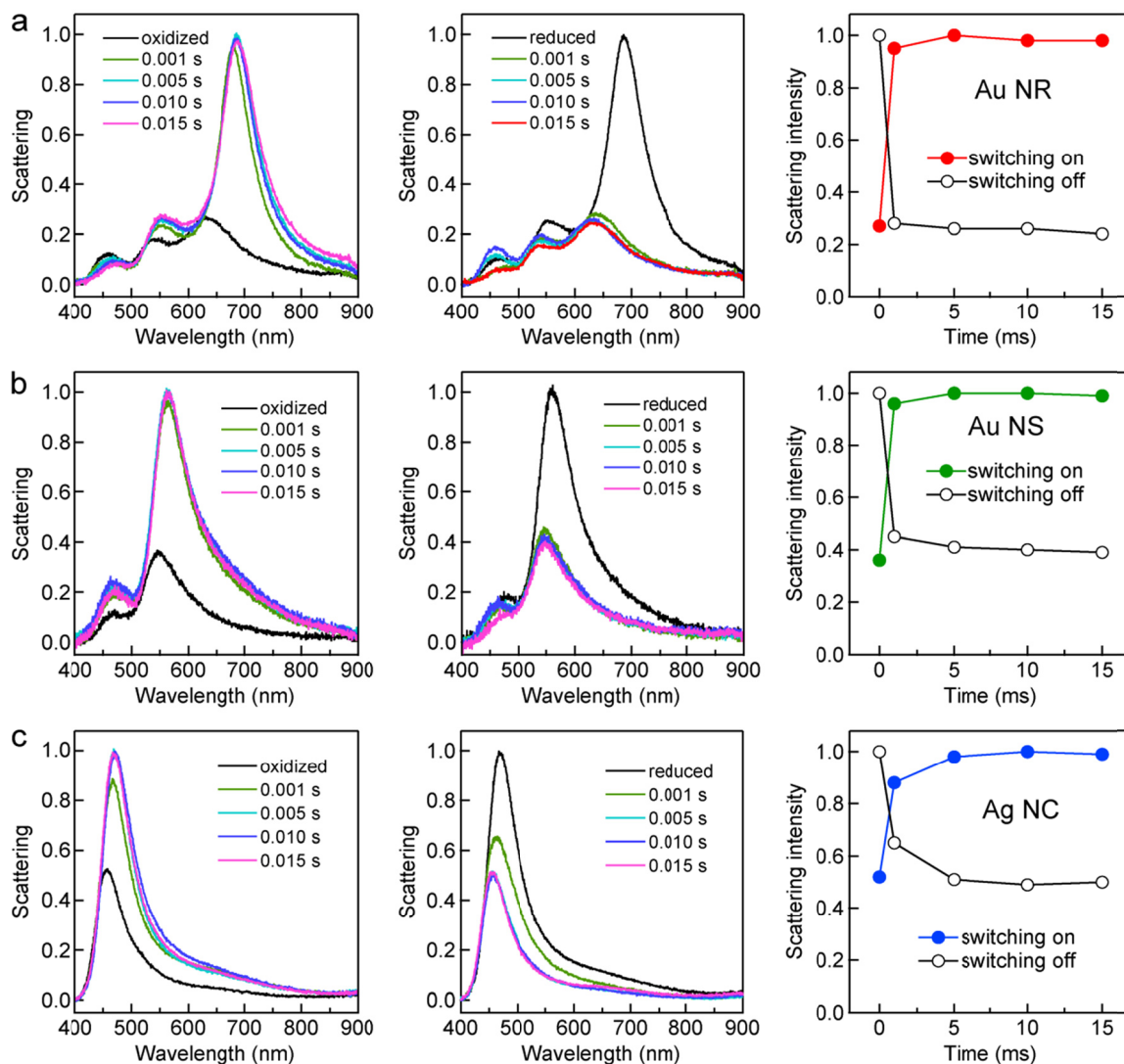
Figure S6. Scattering spectra of the plasmonic blue, green and red colors at their ON and OFF states.

Figure S7. Absorption spectra of a pure PANI film deposited on an ITO substrate in its oxidized and reduced states.
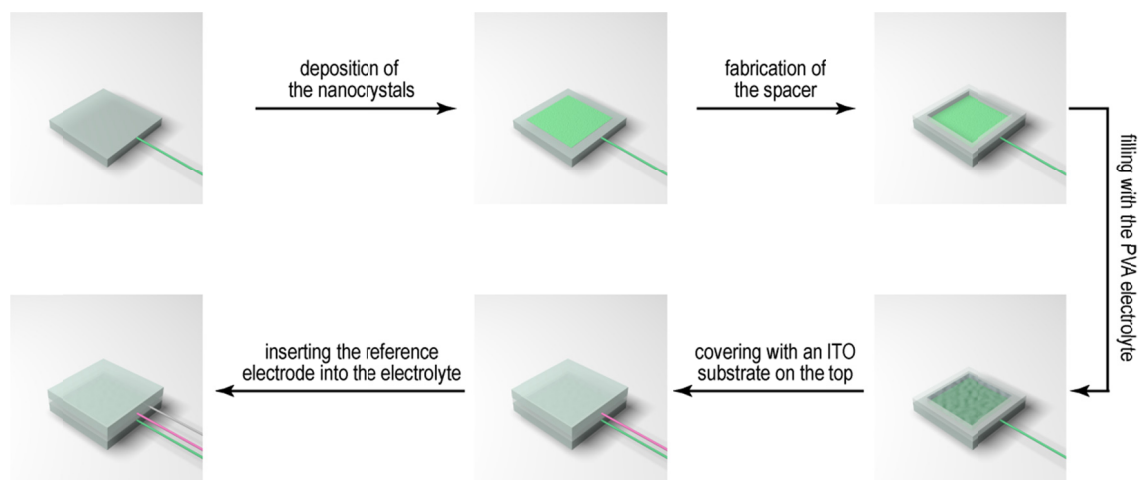
Figure S8. Electrochemical switching durability. (a–c) SEM images of the PANI-coated Au NRs deposited on an ITO substrate before cycling, after 1000 switching cycles and after 10000 switching cycles, respectively.
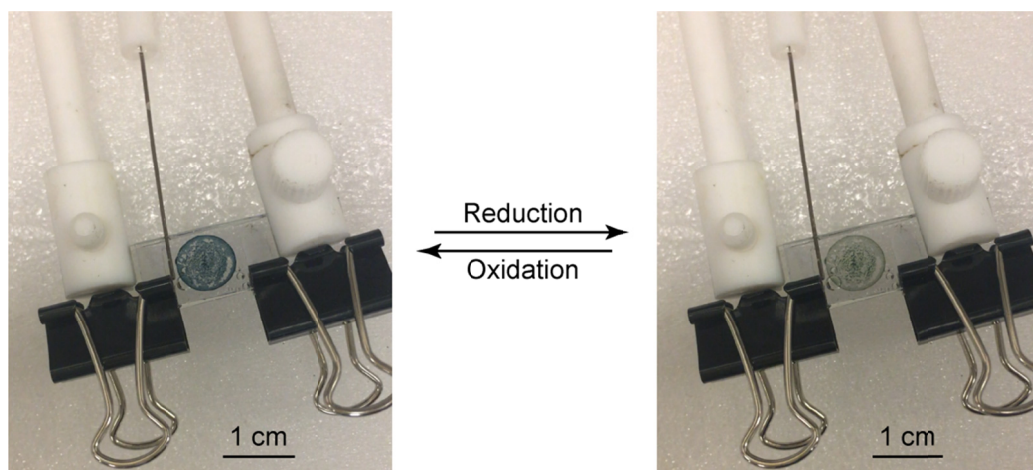
Figure S9. Electrochemical switching rates. (a–c) Scattering spectra of the single PANI-coated Au NR, PANI-coated Au NS and PANI-coated Ag NC, respectively, in the switch-on (left column) and switch-off (middle column) processes, and their scattering intensities as functions of the switching time (right column). The small bump around 465 nm on the scattering spectra in (a) and (b) is caused by the low photon detection efficiency of the optical measurement system in the short-wavelength region.

Figure S10. Schematic illustrating the fabrication of the transparent electrochemical device.

Figure S11. Photographs of the transparent electrochemical switching device with pure PANI deposited on the bottom ITO substrate (working electrode) in the oxidized and reduced states.

REFERENCE

(1)   Hunt, R. W. G.; Pointer, M. R. *Measuring Colour*; John Wiley & Sons: United Kingdom, 2011; pp 99–115.